MATERIALS CHEMISTRY
FRONTIERS

RESEARCH ARTICLE

View Article Online
View Journal | View Issue

Cite this: *Mater. Chem. Front.*, 2018, **2**, 1842

(2-(4-Bromophenyl)ethene-1,1,2-triyl)tribenzene with aggregation induced emission for ablation of HeLa cells†

Jie Yang,[a] Xiaoqing Gu,[a] Wanting Su,[a] Xinyu Hao,[a] Yujie Shi,[a] Liyun Zhao,[b] Dengfeng Zou,[b] Gaowen Yang,[a]* Qiaoyun Li*[a] and Jianhua Zou*[a]

Received 20th June 2018,
Accepted 20th July 2018

DOI: 10.1039/c8qm00304a

rsc.li/frontiers-materials

It is of great importance for a photosensitizer to be soluble in aqueous solutions, while simultaneously remaining highly fluorescent. Towards this goal, (2-(4-bromophenyl)ethene-1,1,2-triyl)tribenzene (denoted as **TPE-Br**) with aggregation induced emission (AIE) was prepared. 1,2-Distearoyl-*sn-glycero*-3-phosphoethanolamine-*N*-[methoxy(polyethyleneglycol)$_{-2000}$] (DSPE-PEG$_{-2000}$) coated **TPE-Br** nanoparticles (NPs) have a strong ability to generate singlet oxygen using singlet oxygen sensor green (SOSG) as a probe and still retain high fluorescence in aqueous solutions. *In vitro* cytotoxicity assays demonstrate that these NPs are able to kill HeLa cells effectively and the half-maximal inhibitory concentration (IC_{50}) is as low as 12 μg mL^{-1}. Furthermore, *in vivo* investigation suggests that **TPE-Br** NPs are able to inhibit the growth of the tumors after irradiation without adverse effects to normal organs, including the heart, liver, spleen, lung and kidney. This indicates the significantly low dark toxicity and excellent biocompatibility of such NPs.

Introduction

Cancer has become the second leading cause of death, following heart disease, and individuals in growing numbers are dying of cancer every year.[1] Traditional therapies, such as surgery, radiation and chemotherapy suffer from negative attributes, such as their invasiveness, being non-targeted and inevitable re-occurrence of cancer.[2–5] Hence, it is urgent to develop more therapies for treatment of cancer. Photodynamic therapy (PDT), is a relatively new therapy, and has attracted increasing attention owing to its non-invasiveness, low cytotoxicity, good biocompatibility, *etc.*[6–11] Photosensitizers play a significant role in PDT, which can generate reactive oxygen species (ROS) under the irradiation of light. However, these photosensitizers (PSs) tend to form π–π stacking aggregates *via* driving forces such as hydrogen bonding, electrostatic interactions, van der Waals interactions, and hydrophobic effects, thus leading to fluorescence quenching.[12–14] The aggregation caused quenching (ACQ) effect limits their potential as fluorescence imaging agents. Therefore, it is considerably significant to develop PSs that can be dispersed in aqueous solutions while remaining highly fluorescent.

Over the past years, significant efforts have been directed towards chemical approaches to prevent ACQ.[15–21] Some fluorophores have enhanced aggregation induced emission (AIE), typically tetraphenylethylene. Such compounds can be dissolved in organic solvents, and their fluorescence becomes stronger in aqueous media because of self-aggregation driven by limited solubility as well as π–π interactions.[22–29] The inferred mechanism of AIE was restriction of intramolecular motion (RIM).[30,31] In solution, the phenyl rings undergo active intramolecular rotational/twisting motions alongside the C–C bonds against the stator upon excitation.

Inspired by these observations, (2-(4-bromophenyl)ethene-1,1,2-triyl)tribenzene (denoted as **TPE-Br**) has been designed and prepared by the condensation reaction of benzophenone and (4-bromophenyl)(phenyl)methanone in the presence of Zn powder and $TiCl_4$. It is expected that this compound's strong rigidity can overcome ACQ and show AIE properties. Moreover, one bromine group has been introduced onto the core in order to enhance singlet oxygen generation by spin orbit coupling (SOC), which is the so-called heavy atom effect. Then, 1,2-distearoyl-*sn-glycero*-3-phospho-ethanolamine-*N*-[methoxy(polyethyleneglycol)$_{-2000}$] (DSPE-PEG$_{-2000}$) coated **TPE-Br** can self-assemble to form nanoparticles (NPs), which have good dispersity in PBS. To further investigate the cytotoxicity of such NPs, HeLa cells have

[a] *Jiangsu Laboratory of Advanced Functional Material, Department of Chemistry and Material Engineering, Changshu Institute of Technology, Changshu 215500, Jiangsu, P. R. China. E-mail: ygwsx@126.com, liqiaoyun61@126.com, zoujh93@126.com*
[b] *School of Pharmacy, Guilin Medical University, Guilin 541004, Guangxi, P. R. China*

† Electronic supplementary information (ESI) available. See DOI: 10.1039/c8qm00304a

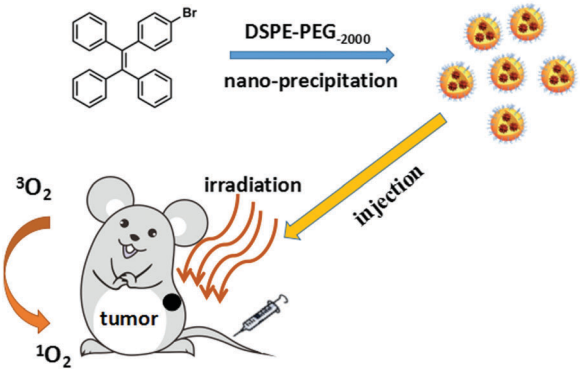

Scheme 1 Illustration of the **TPE-Br** NPs for photodynamic therapy.

been selected. An MTT assay shows that **TPE-Br** NPs, with a low half inhibitory concentration of 12 μg mL^{-1}, are able to kill cells upon light irradiation. Furthermore, *in vivo* studies show that **TPE-Br** NPs are capable of inhibiting the growth of the tumor after irradiation without side effects to the normal tissues (*e.g.*, tissues of heart, liver, spleen, lung and kidney), indicating the significantly low dark toxicity and excellent bio-compatibility of such NPs. Our results show that **TPE-Br** is a potential candidate for photodynamic therapy (Scheme 1).

Experimental

Materials and apparatus

All chemicals were bought from Sigma and used without further purification. ^{1}H NMR was performed on Bruker DRX NMR spectrometer (400 MHz) in $CDCl_3$ at 298 K with solvent residual ($CDCl_3$, δ = 7.26 ppm) as the internal standard. UV-vis spectra were recorded on a spectrophotometer (UV-3600 UV-vis-NIR, Shimadzu, Japan). The fluorescence spectra were measured on a F-4600 spectrometer (HITACHI, Japan). DLS was performed on a 90 Plus particle size analyzer (Brookhaven Instruments, USA). TEM of the nanoparticles were imaged on JEOL JEM-2100 equipment.

Synthesis and characterization of TPE-Br

Under N_2 atmosphere, a mixture of Zn powder (1.12 g, 20 mmol), benzophenone (1.82 g, 10 mmol) and (4-bromophenyl)-(phenyl)methanone (2.60 g, 10 mmol) were dissolved in dried THF (100 mL) and the mixture was cooled to −78 °C. Then, N_2 was purged for 1 h to remove potential oxygen and water impurities. $TiCl_4$ (2.85 g, 15 mmol) was slowly added and the mixture was reacted for 12 h. The mixture was poured to brine and washed with saturated $NaHCO_3$ three times (100 mL). Then, CH_2Cl_2 was used to extract the crude product three times, which was purified by column chromatography on silica gel with CH_2Cl_2/PE (v/v 1 : 2) as the eluant. ^{1}H NMR (500 MHz, DMSO) 7.24–7.21 (2H, d), 7.14–7.06 (9H, m), 7.04–6.97 (6H, m), 6.91–6.85 (2H, d); elemental analysis for $C_{26}H_{19}Br$: C, 75.92; H, 4.66; found C, 75.73, H, 4.52; MS (ESI): calcd m/z = 410.07; found m/z = 410.35.

Preparation of TPE-Br nanoparticles

The nanoparticles of **TPE-Br** were prepared by nanoprecipitation with DSPE-PEG$_{2000}$. 1,2-Distearoyl-*sn-glycero*-3-phospho-ethanolamine-*N*-[methoxy (polyethyleneglycol)$_{2000}$] (1 mg) and **TPE-Br** (5 mg) were dissolved in tetrahydrofuran (THF, 1 mL) under ultrasonication. Then, 200 μL of this solution was injected into PBS under vigorous stirring at room temperature. After the mixture was stirred for 30 min, THF was removed by nitrogen bubbling. DSPE-PEG$_{2000}$ coated **TPE-Br** NPs in solution were obtained by centrifugation.

Cell culture and MTT assay

HeLa cell lines were cultured in a regular growth medium comprising Dulbecco's modified Eagle's medium (DMEM, Gibco) with 10% fetal bovine serum (FBS) under an atmosphere of 5% CO_2 at 37 °C. Cell viability assays of the **TPE-Br** NPs were first dissolved in distilled water, which were diluted with DMEM to various concentrations (0–20 μg mL^{-1}) and put in the 96-well plate. Then, the plate was irradiated with a xenon lamp (30 mW cm^{-2}) for 5 minutes. Cell viability was determined by colorimetric 3-(4,5-dimethylthiazol-2-yl)-2,5-diphenyltetrazolium bromide (MTT) assay. MTT in distilled water (5 mg mL^{-1}, 20 μL) was added to each well, followed by incubation for 4 h under the same conditions at 37 °C. Then, the solution was discarded, followed by the addition of DMSO (200 μL). At ambient temperature, the absorbance below 490 nm was measured on a Bio-Tek microplate reader. The cell viability of the control group (without **TPE-Br** NPs) was considered as 100%. The relative cell viability was then determined by the following equation: viability (%) = $\{\sum[(A_i/A_{control}) \times 100]\}/n$, where A_i is the absorbance of the corresponding data (i = 1, 2, 3, 4, 5) and $A_{control}$ is the average absorbance in control wells.

Cellular uptake and fluorescence imaging of cellular ROS

HeLa cells were incubated with DSPE-PEG$_{2000}$ coated **TPE-Br** NPs (12 μg mL^{-1}, 2 mL) in a confocal dish in the dark for 24 h. Then, the solution was discarded and the cells were washed with PBS three times (1 mL), followed by the addition of 1 mL polyoxymethylene for 25 min. Then, polyoxymethylene was discarded and the cells were washed with PBS three times (1 mL). The sample incubated with **TPE-Br** NPs for 24 h, was further cultured with 10 μM of 2,7-dichlorodihydrofluorescein diacetate (DCF-DA) for another 5 min. Subsequently, it was washed with PBS three times (1 mL). This sample was irradiated by Xenon lamp (>510 nm, 30 mW cm^{-2}) for 3 minutes. The fluorescence images were observed with a Olympus IX 70 inverted microscope. The samples incubated with **TPE-Br** NPs for 24 h were excited at a wavelength of 433 nm and the fluorescence spectrum was recorded from 450 to 600 nm. The sample incubated with DCF-DA under irradiation was excited with a 488 nm laser and fluorescence was recorded from 490 to 600 nm.

In vivo tumor treatment histology examination

The study complies with all institutional and national guidelines, and was approved by the Chinese laws. The protocol was

approved by Animal Center of Guilin Medical University (SCXK2007-001). In total, 12 nude mice were purchased and then, each mice was injected with HeLa cells as the tumor source in the armpit. When the tumor volume reached about 100 mm^3, the mice were divided into 3 groups randomly. For the control group, the mice were intravenously injected with saline, while the other groups were injected with **TPE-Br** NPs (60 μg mL^{-1}, 100 μL) in PBS solution. After 4 h, the mice groups with irradiation were irradiated by Xenon lamp for 10 minutes, while the mice in the control and without irradiation groups were not irradiated. The process was conducted for twenty days, and the tumor volume and body weight of mice were recorded every two days. Subsequently, these nude mice were killed, followed by the histological analysis. The main organs (heart, liver, spleen, lung, kidney) and the tumor from each mouse was isolated and fixed in 4% formaldehyde solution. After dehydration, they were embedded in paraffin cassettes and stained with hematoxylin and eosin (H&E); the images were recorded on a microscope.

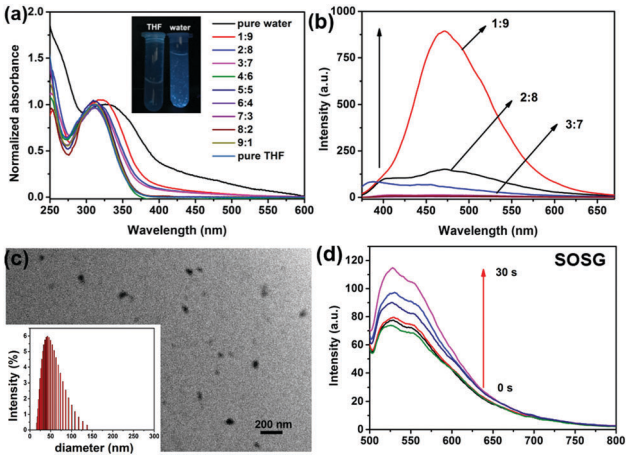

Fig. 1 (a) Normalized absorbance of **TPE-Br** in THF with different fractions of water (THF/water: (v/v) from pure water, 1 : 9, 2 : 8 to 9 : 1, pure THF) (b) fluorescence intensity of **TPE-Br** in THF/water with different fractions (v/v THF/water from 1 : 9 to 9 : 1); (c) TEM and DLS of DSPE-PEG_{2000} coated **TPE-Br** NPs; (d) ROS generation of **TPE-Br** NPs with SOSG as a probe in water.

Results and discussion

Synthesis and characterization of TPE-Br and NPs

The absorbance of **TPE-Br** and its nanoparticles (NPs) were measured. **TPE-Br** in THF shows the peak at 305 nm. With an increase in fraction of water, a red shift in the absorbance was observed, and the peak of the NPs moved to 345 nm. Also, the absorbance of NPs in water becomes broader than that in DCM, which may be caused by their aggregation in water. In the fluorescence spectra, a large Stokes shift of 105 nm was observed, indicating the potential AIE of such NPs. To further investigate the AIE characteristic of **TPE-Br** NPs, the fluorescence at different THF/water ratios was reported. As shown in Fig. 1b, with an increase in fraction of water, the fluorescence of **TPE-Br** jumps sharply, which is characteristic of AIE. The absolute quantum yield of **TPE-Br** in THF is 1.2%, while that of DSPE-PEG_{2000} coated **TPE-Br** NPs is 32.4%. Transmission electron microscope (TEM) of **TPE-Br** NPs demonstrates that it can self-assemble to form nanoparticles with mean diameters of approximately 70 nm, which is consistent with the dynamic light scattering (DLS) results. Since singlet oxygen generation in aqueous solution is essential for PDT, SOSG (singlet oxygen sensor green) was used as a probe. Fig. 1d shows the fluorescence enhancement of SOSG with light irradiation, indicating the strong singlet oxygen generation ability of such NPs.

MTT assay, cellular uptake and ROS generation *in vitro*

As shown in Fig. 2, to evaluate the suitability of **TPE-Br** NPs for cell imaging *in vitro*, cellular uptake of DSPE-PEG_{2000} coated **TPE-Br** NPs was measured. **TPE-Br** NPs could be used as an agent for cell imaging because green fluorescence was observed. 2′,7′-Dichlorofluorescein diacetate (DCF-DA) probe was selected to detect singlet oxygen generation under excitation at 488 nm (the excitation wavelength of DCF-DA). It is found that **TPE-Br** NPs are able to generate singlet oxygen efficiently *in vitro* due to the observed strong green fluorescence (Fig. 2).

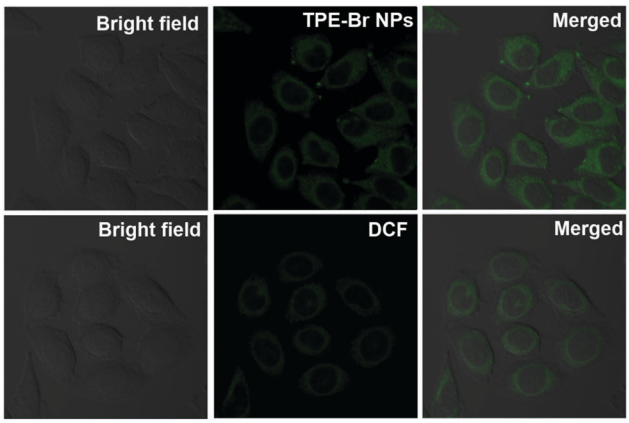

Fig. 2 Cellular uptake of **TPE-Br** NPs in HeLa cells and ROS generation *in vitro* with DCF-DA as a probe.

To further investigate the phototherapy efficacy of **TPE-Br** NPs, an MTT assay was performed. First, high phototoxicity is fundamental for photodynamic therapy. It can be seen that cell viability has been drastically suppressed by increasing the concentration of the NPs, and the half inhibitory concentration (IC_{50}) is as low as 12 μg mL^{-1}, which is superior to that of ETTDA NPs (40 μg mL^{-1}) (ETTDA = 4,4′,4″,4‴-(ethene-1,1,2,2-tetrayl)tetrakis(*N*,*N*-diethylaniline)).[32] Moreover, low dark toxicity is crucial for a photosensitizer to minimize the side effects on normal tissues. The dark toxicity of such NPs can be almost neglected because the cell viability remains at a high level.

In vivo phototherapy efficacy of TPE-Br NPs

The PDT efficacy of **TPE-Br** NPs *in vivo* was further investigated using 12 HeLa tumor-bearing nude mice, which were divided into three groups randomly. As shown in Fig. 3b, the tumor volume of the control group, which was recorded every two days,

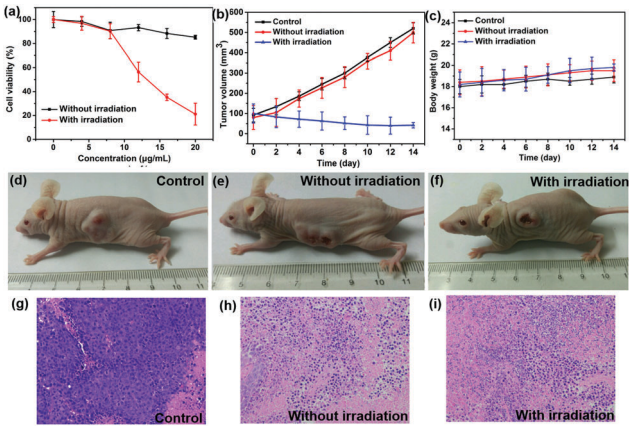

Fig. 3 (a) MTT assay of **TPE-Br** NPs on HeLa cells; (b) tumor volume change of the three groups; (c) body weight change of the groups; (d–f) picture of the mice in control, no illumination and illumination groups; (g–i) H&E stained picture of the three groups.

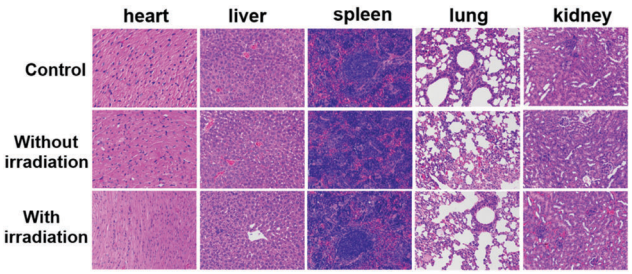

Fig. 4 H&E stained picture of the normal organs, including heart, liver, spleen, lung and kidney.

increases quickly, while that of the illumination-free group rises slightly slowly due to the fact that irradiation by room light inevitably generates $^1O_2$ that inhibits tumor growth. In case of the illumination group, the tumor volume remains almost unchanged during treatment. The body weight of the mice in the control group decreases, while those in the other two groups increase, demonstrating the low dark toxicity and good bio-compatibility of **TPE-Br** NPs (Fig. 3c). The hematoxylin and eosin (H&E)-stained images of the tumor histologic section of control and no illumination group (Fig. 3g–i) shows that the nucleus of HeLa cells remain almost unchanged, again suggesting low dark toxicity. After treatment, these mice were sacrificed and the tumors are shown in Fig. S1 (ESI†). No significant difference between the images of the main organs (heart, liver, spleen, lung, kidney) (Fig. 4) in non-illuminated and illuminated groups are observed, indicating that **TPE-Br** NPs cause negligible damage to normal tissues. However, in case of the illumination groups, the nuclei of the cells are distorted, suggesting the phototherapy efficacy of such NPs.[33,34]

Conclusions

In summary, **TPE-Br** with aggregation induced emission has been prepared. DSPE-PEG$_{-2000}$ coated **TPE-Br** NPs demonstrate high fluorescence and produce singlet oxygen in an aqueous solution. *In vitro* studies show that these NPs can used as a cell imaging agent and have a low IC_{50} of only 12 μg mL^{-1}. Furthermore, DSPE-PEG$_{-2000}$ coated **TPE-Br** NPs can effectively inhibit the growth of tumors while normal tissues suffer no damage, indicating the high phototoxicity, low dark toxicity and good bio-compatibility of such NPs. Further investigations are currently underway in our group.

Conflicts of interest

There are no conflicts to declare.

Acknowledgements

The authors acknowledge financial support from the Natural Science Foundation of Jiangsu Province (Grant No. BK2012210), the Natural Science Foundation of the Jiangsu Higher Education Institutions of China (Grant No. 10KJB430001) and the Opening Fund of Jiangsu Key Laboratory of Advanced Functional Materials (Grant No. 12KFJJ010).

Notes and references

1 R. L. Siegel, K. D. Miller and A. Jemal, *Ca-Cancer J. Clin.*, 2018, **68**, 7–30.
2 N. Shivran, M. Tyagi, S. Mula, P. Gupta, B. Saha, B. S. Patro and S. Chattopadhyay, *Eur. J. Med. Chem.*, 2016, **122**, 352–365.
3 M. Laine, N. A. Barbosa, A. Kochel, B. Osiecka, G. Szewczyk, T. Sarna, P. Ziółkowski, R. Wieczorek and A. Filarowski, *Sens. Actuators, B*, 2017, **238**, 548–555.
4 X. Song, Q. Chen and Z. Liu, *Nano Res.*, 2014, **8**, 340–354.
5 A. Carija, N. Puizina-Ivic, D. Vukovic, L. Miric Kovacevic and V. Capkun, *Photodiagn. Photodyn. Ther.*, 2016, **16**, 60–65.
6 A. Kamkaew, S. H. Lim, H. B. Lee, L. V. Kiew, L. Y. Chung and K. Burgess, *Chem. Soc. Rev.*, 2013, **42**, 77–88.
7 C. C. Chang, M. C. Hsieh, J. C. Lin and T. C. Chang, *Biomaterials*, 2012, **33**, 897–906.
8 J. Schmitt, V. Heitz, A. Sour, F. Bolze, H. Ftouni, J. F. Nicoud, L. Flamigni and B. Ventura, *Angew. Chem., Int. Ed.*, 2015, **54**, 169–173.
9 E. Secret, M. Maynadier, A. Gallud, A. Chaix, E. Bouffard, M. Gary-Bobo, N. Marcotte, O. Mongin, K. El Cheikh, V. Hugues, M. Auffan, C. Frochot, A. Morere, P. Maillard, M. Blanchard-Desce, M. J. Sailor, M. Garcia, J. O. Durand and F. Cunin, *Adv. Mater.*, 2014, **26**, 7643–7648.
10 M. Li, Y. Gao, Y. Y. Yuan, Y. Z. Wu, Z. F. Song, B. Z. Tang, B. Liu and Q. C. Zheng, *ACS Nano*, 2017, **11**, 3922–3932.
11 X. L. Cai, C. J. Zhang, F. T. W. Lim, S. J. Chan, A. Bandla, C. K. Chuan, F. Hu, S. D. Xu, N. V. Thakor, L. D. Liao and B. Liu, *Small*, 2016, **12**, 6576–6585.
12 C. A. Hunter and M. K. J. Sanders, *Photochem. Photobiol.*, 2013, **88**, 1011–1019.

13 C. A. Hunter and J. K. M. Sanders, *J. Am. Chem. Soc.*, 1990, **112**, 5525–5534.
14 U. Siggel, U. Bindig, C. Endisch, T. Komatsu, E. Tsuchida, E. Voigt and J. H. Fuhrhop, *Ber. Bunsenges. Phys. Chem.*, 1996, **100**, 2070–2075.
15 G. X. Feng, R. T. K. Kwok, B. Z. Tang and B. Liu, *Appl. Phys. Rev.*, 2017, **4**, 021307.
16 E. Sen, K. Meral and S. Atılgan, *Chem. – Eur. J.*, 2016, **22**, 736–745.
17 Z. Y. Fan, D. D. Li, X. Yu, Y. P. Zhang, Y. Cai, J. J. Jin and J. H. Yu, *Chem. – Eur. J.*, 2016, **22**, 3681–3685.
18 A. T. Han, H. M. Wang, R. T. K. Kwok, S. L. Ji, J. Li, D. L. Kong, B. Z. Tang, B. Liu, Z. M. Yang and D. Ding, *Anal. Chem.*, 2016, **88**, 3872–3878.
19 M. Li, Y. Gao, Y. Y. Yuan, Y. Z. Wu, Z. F. Song, B. Z. Tang, B. Liu and Q. C. Zheng, *ACS Nano*, 2017, **11**, 3922–3932.
20 E. J. Wang, E. G. Zhao, Y. N. Hong, J. W. Y. Lam and B. Z. Tang, *J. Mater. Chem. B*, 2014, **2**, 2013–2019.
21 S. D. Xu, Y. Y. Yuan, X. L. Cai, C. J. Zhang, F. Hu, J. Liang, G. X. Zhang, D. Q. Zhang and B. Liu, *Chem. Sci.*, 2015, **6**, 5824–5830.
22 Y. Y. Yuan, C. J. Zhang, M. Gao, R. Y. Zhang, B. Z. Tang and B. Liu, *Angew. Chem., Int. Ed.*, 2015, **54**, 1780–1786.
23 Y. Y. Yuan, C. J. Zhang, S. D. Xu and B. Liu, *Chem. Sci.*, 2016, **7**, 1862–1866.
24 Z. F. Chang, L. M. Jing, B. Chen, M. S. Zhang, X. L. Cai, J. J. Liu, Y. C. Ye, X. D. Lou, Z. J. Zhao, B. Liu, J. L. Wang and B. Z. Tang, *Chem. Sci.*, 2016, **7**, 4527–4536.
25 X. Y. Gao, G. X. Feng, P. N. Manghnani, F. Hu, N. Jiang, J. Z. Liu, B. Liu, J. Z. Sun and B. Z. Tang, *Chem. Commun.*, 2017, **53**, 1653–1656.
26 Y. Y. Yuan, C. J. Zhang, R. T. K. Kwok, D. Mao, B. Z. Tang and B. Liu, *Chem. Sci.*, 2017, **8**, 2723–2728.
27 X. L. Cai, C. J. Zhang, F. T. Wei Lim, S. J. Chan, A. Bandla, C. K. Chuan, F. Hu, S. D. Xu, N. V. Thakor, L. D. Liao and B. Liu, *Small*, 2016, **12**, 6576–6585.
28 B. B. Gu, W. B. Wu, G. X. Xu, G. X. Feng, F. Yin, P. H. Joo Chong, J. L. Qu, K. T. Yong and B. Liu, *Adv. Mater.*, 2017, 1701076.
29 C. J. Zhang, G. X. Feng, S. D. Xu, Z. S. Zhu, X. M. Lu, J. Wu and B. Liu, *Angew. Chem., Int. Ed.*, 2016, **55**, 6192–6196.
30 M. Yamaguchi, S. Ito, A. Hirose, K. Tanaka and Y. Chujo, *Mater. Chem. Front.*, 2017, **1**, 1573–1579.
31 W. Zheng, G. Yang, S. T. Jiang, N. N. Shao, G. Q. Yin, L. Xu, X. P. Li, G. S. Chen and H. B. Yang, *Mater. Chem. Front.*, 2017, **1**, 1823–1828.
32 Q. Y. Li, Z. Y. Yang, W. T. Su, D. Y. Chen, G. W. Yang and D. F. Zou, *ChemistrySelect*, 2018, **3**, 2332–2335.
33 H. He, S. S. Ji, Y. He, A. J. Zhu, Y. L. Zou, Y. B. Deng, H. T. Ke, H. Yang, Y. L. Zhao, Z. Q. Guo and H. B. Chen, *Adv. Mater.*, 2017, **29**, 1606690.
34 L. Huang, Z. J. Li, Y. Zhao, J. Y. Yang, Y. C. Yang, A. I. Pendharkar, Y. W. Zhang, S. Kelmar, L. Y. Chen, W. T. Wu, J. Z. Zhao and G. Han, *Adv. Mater.*, 2017, **29**, 1604789.

